Numerical solution of coupled KdV systems of Boussinesq equations: I. The numerical scheme and existence of generalized solitary waves

J. L. Bona [a,1], V. A. Dougalis [b,c] and D. E. Mitsotakis [b,c]

[a] *Department of Mathematics, Statistics and Computer Science, University of Illinois, Chicago, IL 60607, USA*
[b] *Department of Mathematics, University of Athens, 15784 Zographou, Greece*
[c] *Institute of Applied and Computational Mathematics, FO.R.T.H., P.O. Box 1527, 71110 Heraklion, Greece*

Abstract

We consider some Boussinesq systems of water wave theory, which are of coupled KdV type. After a brief review of the theory of existence-uniqueness of solutions of the associated initial-value problems, we turn to the numerical solution of their initial- and periodic boundary-value problems by unconditionally stable, highly accurate methods that use Galerkin/finite element type schemes with periodic splines for the spatial and the two-stage Gauss-Legendre implicit Runge-Kutta method for the temporal discretization. These systems are shown to possess generalized solitary wave solutions, wherein the main solitary wave pulse decays to small amplitude periodic solutions. Solutions of this type are constructed and studied by numerical means.

Key words: Boussinesq systems, coupled KdV systems, generalized solitary waves, Galerkin/finite element method, splines, Gauss-Legendre implicit Runge-Kutta method

1. Introduction

The *coupled Korteweg-de Vries* (KdV) system of equations is a system of Boussinesq type, [4], that models the one-dimensional, bidirectional propagation of surface water waves of small amplitude and large wavelength when the Stokes number is $O(1)$. In dimensionless, unscaled variables it is written for $x \in \mathbb{R}$, $t > 0$, as

$$\begin{aligned} &\eta_t + u_x + (\eta u)_x + \tfrac{1}{6} u_{xxx} = 0, \\ &u_t + \eta_x + u u_x + \tfrac{1}{6} \eta_{xxx} = 0, \end{aligned} \tag{1}$$

Email addresses: bona@math.uic.edu (J. L. Bona), dmitsot@math.uoa.gr (D. E. Mitsotakis).
[1] Corresponding author

where $\eta = \eta(x,t)$ represents the elevation of the free surface and $u = u(x,t)$ the horizontal velocity at some depth. The initial-value problem of (1) with initial data $\eta(x,0) = \eta_0(x)$, $u(x,0) = u_0(x)$, $x \in \mathbb{R}$, is linearly well-posed for $(\eta, u) \in H^s \times H^s$ for $s \geq 0$ but is ill-posed in L^p for $p \neq 2$, cf. [4]. For the nonlinear system, it was shown in [5] that if $(\eta_0, u_0) \in H^s \times H^s$ for $s > 3/4$, then there exist $T > 0$ and a unique solution of (1) such that $(\eta, u) \in C(0,T;H^s)^2$, $(\eta_t, u_t) \in C(0,T;H^{s-3})^2$. Moreover, it is readily seen that the solution of (1) conserves the quantities $I_1 = \int_{-\infty}^{\infty} u dx$, $I_2 = \int_{-\infty}^{\infty} \eta dx$, $I_3 = \int_{-\infty}^{\infty} u\eta dx$, and the Hamiltonian $H = \int_{-\infty}^{\infty} \left(\frac{1}{6}\eta_x^2 + \frac{1}{6}u_x^2 - \eta^2 - u^2 - u^2\eta\right) dx$.

Related to (1) is the so-called *symmetric coupled KdV system*, [6], which is written in the form

$$\begin{aligned} &\eta_t + u_x + \tfrac{1}{2}(\eta u)_x + \tfrac{1}{6}u_{xxx} = 0, \\ &u_t + \eta_x + \tfrac{1}{2}\eta\eta_x + \tfrac{3}{2}uu_x + \tfrac{1}{6}\eta_{xxx} = 0, \end{aligned} \tag{2}$$

and which reduces to a symmetric hyperbolic system when the dispersive terms (the third-order derivatives) are dropped. A local existence-uniqueness theory holds for the initial-value problem for (2) as well. Specifically, it is shown in [6] that for $(\eta_0, u_0) \in H^s \times H^s$, $s > 3/2$, there exists $T > 0$ and a unique solution of (2) such that $(\eta, u) \in C(0,T;H^s)^2$. Note that the (2) is L^2 conservative, as the quantity $\int_{-\infty}^{\infty} \left(\eta^2 + u^2\right) dx$ is invariant.

Another related system is a more general version of (1), namely

$$\begin{aligned} &\eta_t + u_x + (\eta u)_x + \tfrac{1}{6}u_{xxx} = 0, \\ &u_t + \eta_x + uu_x + (\tfrac{1}{6} - \tau)\eta_{xxx} = 0, \end{aligned} \tag{3}$$

which contains a surface tension parameter, the Bond number τ, see e.g. [9]. For $\tau < 1/6$ this system has a local existence-uniqueness theory similar to that of (1).

In this note we study (1)–(3) numerically. The initial- and periodic boundary-value problem for these systems, when discretized in space (we use the standard Galerkin/finite element method with smooth splines on a uniform mesh) yields highly stiff systems of ordinary differential equations. Hence, it is not efficient to use explicit schemes for their temporal discretization. (The latter work well with the nonstiff Bona-Smith and 'classical' Boussinesq systems, [1].) We resort instead to the two-stage implicit Runge-Kutta scheme of the Gauss-Legendre type, which is of fourth order accuracy and possesses favorable nonlinear stability properties. The resulting nonlinear system of equations is linearized at each time step by Newton's method coupled with appropriate "inner" iterative schemes for solving the attendant linear systems efficiently, in the spirit of the analogous scheme for the scalar KdV equation in [7]. The fully discrete scheme obtained in this way is unconditionally stable and highly accurate; its construction is outlined in Section 2 and the scheme is tested for accuracy in Section 3.

As approximations to the Euler equations of water wave theory the systems (1)–(3) could have been reasonably expected to possess solitary wave solutions. We show in Section 4, by appeal to Lombardi's theory, cf. [11] and the references therein, that (1) and (2) do not possess solitary wave solutions in the usual sense but have *generalized solitary waves*, which, instead of decaying to zero as $|x| \to \infty$, are homoclinic to periodic solutions of small amplitude (ripples). Such generalized solitary waves have been shown to exist in cases of gravity-capillary surface wave models and also for various other model equations and systems arising in water wave theory; see e.g. [2], [10]–[12], [14], [15]. We construct generalized solitary waves for (1)–(3) by solving numerically periodic boundary-value problems for the nonlinear o.d.e. systems that travelling wave solutions of these systems satisfy. The resulting wave profiles are indeed of the above-described form and travel with constant speed and shape when inserted as initial values to the evolution code of Sections 2 and 3. The system (3) possesses solitary waves of the usual type (for $\frac{1}{12} < \tau < \frac{1}{6}$) and also generalized solitary waves.

The present paper is accompanied by a second one by the same authors, in which the evolution code is used in a numerical study of the generation, interaction and stability of the generalized solitary waves of (1) and (2).

2. The numerical method

Let $r \geq 3$ and consider the space $S_h = S_h^r$ of periodic smooth splines of order r (degree $r-1$) on $[a,b]$, on a uniform mesh with meshlength $h = (b-a)/N$. The standard Galerkin semidiscretization of the initial-periodic value problem for (1) on $[a,b]$ is a map $(\eta_h, u_h) : [0,T] \to S_h \times S_h$ satisfying

$$\begin{aligned} (\eta_{ht}, \chi) &= -(u_{hx} + \eta_{hx} u_h + \eta_h u_{hx}, \chi) + \tfrac{1}{6}(u_{hxx}, \chi_x), \ \text{ for all } \ \chi \in S_h, \\ (u_{ht}, \psi) &= -(\eta_{hx} + u_{hx} u_h, \psi) + \tfrac{1}{6}(\eta_{hxx}, \psi_x), \ \text{ for all } \ \psi \in S_h, \end{aligned} \tag{4}$$

and for which $\eta_h(0) = \Pi_h \eta_0$ and $u_h(0) = \Pi_h u_0$, where Π_h denotes any one of the projections such as interpolant, L_2-projection, etc., such that for smooth, periodic v there holds that $\|\Pi_h v - v\| \leq c h^r$ for some constant c independent of h. Here $(\cdot,\cdot)$, $\|\cdot\|$ denote, respectively, the L^2 inner product and norm on $[a,b]$. Define $F_1, F_2 : S_h \times S_h \to S_h$ by requiring that

$$\begin{aligned} (F_1(\eta,u), \chi) &= -(u_x + \eta_x u + \eta u_x, \chi) + \tfrac{1}{6}(u_{xx}, \chi_x), \ \text{ for all } \ \chi \in S_h, \\ (F_2(\eta,u), \psi) &= -(\eta_x + u u_x, \psi) + \tfrac{1}{6}(\eta_{xx}, \psi_x), \ \text{ for all } \ \psi \in S_h. \end{aligned} \tag{5}$$

With this notation, the semidiscretization is a map $(\eta_h, u_h) : [0,T] \to S_h \times S_h$ satisfying

$$\eta_{ht} = F_1(\eta_h, u_h), \quad u_{ht} = F_2(\eta_h, u_h), \tag{6}$$

for all $t \in [0,T]$, and for which $\eta_h(0) = \Pi_h \eta_0$ and $u_h(0) = \Pi_h u_0$.

We consider the map $Q : S_h \times S_h \to S_h$ defined for $v, w \in S_h$ as $(Q(v,w), \chi) = (vw, \chi')$, for all $\chi \in S_h$. We denote $Q(v) = Q(v,v)$. Let $\Theta : S_h \to S_h$ be the linear operator defined for $v \in S_h$ by $(\Theta v, \chi) = \frac{1}{6}(v_{xx}, \chi') - (v_x, \chi)$ for all $\chi \in S_h$. Using this notation we may write the system (6) in the form

$$\eta_{ht} = F_1(\eta_h, u_h) = Q(u_h, \eta_h) + \Theta u_h, \quad u_{ht} = F_2(\eta_h, u_h) = \frac{1}{2} Q(u_h) + \Theta \eta_h. \tag{7}$$

We shall discretize (7) in the temporal variable by the 2-stage Gauss-Legendre implicit Runge-Kutta method, which corresponds to the table

$$\begin{array}{cc|c} a_{11} & a_{12} & \tau_1 \\ a_{21} & a_{22} & \tau_2 \\ \hline b_1 & b_2 & \end{array} \quad = \quad \begin{array}{cc|c} \frac{1}{4} & \frac{1}{4} - \frac{1}{2\sqrt{3}} & \frac{1}{2} - \frac{1}{2\sqrt{3}} \\ \frac{1}{4} + \frac{1}{2\sqrt{3}} & \frac{1}{4} & \frac{1}{2} + \frac{1}{2\sqrt{3}} \\ \hline \frac{1}{2} & \frac{1}{2} & \end{array}.$$

Specifically, let $t^n = nk$, $n = 0, 1, \ldots, J$, where $T = Jk$. We seek H^n, U^n, by way of the intermediate stages $H^{n,i}, U^{n,i}$ in S_h, $i = 1, 2$, which are the solutions of the 2×2 system of nonlinear equations

$$H^{n,i} = H^n + k \sum_{j=1}^{2} a_{ij} F_1(H^{n,j}, U^{n,j}), \quad U^{n,i} = U^n + k \sum_{j=1}^{2} a_{ij} F_2(H^{n,j}, U^{n,j}), \quad i = 1, 2, \tag{8}$$

using the formulas

$$H^{n+1} = H^n + \sum_{j=1}^{2} b_j F_1(H^{n,j}, U^{n,j}), \quad U^{n+1} = U^n + \sum_{j=1}^{2} b_j F_2(H^{n,j}, U^{n,j}). \tag{9}$$

At each time step we solve the nonlinear system represented by (8) using Newton's method as follows. Given $n \geqslant 0$, let $H_0^{n,i}, U_0^{n,i} \in S_h$, $i = 1, 2$, be an accurate enough initial guess for $H^{n,i}, U^{n,i}$, respectively. Then the iterates of Newton's method for (8) (called the *outer* iterates) $H_j^{n,i}, U_j^{n,i}$, $j = 1, 2, \ldots$, satisfy the linear system

$$\begin{aligned} H_{j+1}^{n,i} \; & -k \textstyle\sum_{m=1}^{2} a_{im} \left(\Theta U_{j+1}^{n,m} + Q(H_{j+1}^{n,m}, U_j^{n,m}) + Q(H_j^{n,m}, U_{j+1}^{n,m}) \right) \\ & = H^n - k \textstyle\sum_{m=1}^{2} a_{im} Q(H_j^{n,m}, U_j^{n,m}), \quad i = 1, 2, \end{aligned} \tag{10}$$

$$U_{j+1}^{n,i} - k \sum_{m=1}^{2} a_{im} \left(\Theta H_{j+1}^{n,m} + Q(U_{j+1}^{n,m}, U_j^{n,m}) \right) = U^n - k \sum_{m=1}^{2} a_{im} \frac{1}{2} Q(U_j^{n,m}), \quad i = 1, 2. \tag{11}$$

To solve efficiently the linear system represented by these equations, we add equation (10), $i = 1$ to (11), i=1, and (10), $i = 2$ to (11), i=2. We also subtract equation (11), $i = 1$ from (10), $i = 1$, and equation (11), $i = 2$ from (10), $i = 2$, producing four new equations which we write in operator form as a 2×2 block-diagonal linear system

$$\left(\begin{array}{c|c} A_1 & 0 \\ \hline 0 & A_2 \end{array} \right) \begin{pmatrix} H_{j+1}^{n,1} + U_{j+1}^{n,1} \\ \hline H_{j+1}^{n,2} + U_{j+1}^{n,2} \\ \hline H_{j+1}^{n,1} - U_{j+1}^{n,1} \\ H_{j+1}^{n,2} - U_{j+1}^{n,2} \end{pmatrix} + \begin{pmatrix} \mathbf{b} \\ \hline \mathbf{b} \end{pmatrix} = \begin{pmatrix} r_1 \\ \hline r_2 \\ \hline q_1 \\ q_2 \end{pmatrix},$$

where

$$A_1 = \begin{pmatrix} I - ka_{11} \left(\Theta \cdot + Q(\cdot, U_j^{n,1}) \right) & -ka_{12} \left(\Theta \cdot + Q(\cdot, U_j^{n,2}) \right) \\ -ka_{21} \left(\Theta \cdot + Q(\cdot, U_j^{n,1}) \right) & I - ka_{22} \left(\Theta \cdot + Q(\cdot, U_j^{n,2}) \right) \end{pmatrix},$$

$$A_2 = \begin{pmatrix} I - ka_{11} \left(-\Theta \cdot + Q(\cdot, U_j^{n,1}) \right) & -ka_{12} \left(-\Theta \cdot + Q(\cdot, U_j^{n,2}) \right) \\ -ka_{21} \left(-\Theta \cdot + Q(\cdot, U_j^{n,1}) \right) & I - ka_{22} \left(-\Theta \cdot + Q(\cdot, U_j^{n,2}) \right) \end{pmatrix},$$

$$\mathbf{b} = \begin{pmatrix} -ka_{11} Q(H_j^{n,1}, U_{j+1}^{n,1}) - ka_{12} Q(H_j^{n,2}, U_{j+1}^{n,2}) \\ -ka_{21} Q(H_j^{n,1}, U_{j+1}^{n,1}) - ka_{22} Q(H_j^{n,2}, U_{j+1}^{n,2}) \end{pmatrix},$$

$$r_i = H^n + U^n - k \sum_{m=1}^{2} a_{im} \left(Q(H_j^{n,m}, U_j^{n,m}) + \frac{1}{2} Q(U_j^{n,m}) \right), \quad i = 1, 2$$

$$q_i = H^n - U^n - k \sum_{m=1}^{2} a_{im} \left(Q(H_j^{n,m}, U_j^{n,m}) - \frac{1}{2} Q(U_j^{n,m}) \right), \quad i = 1, 2$$

The above system is split into two 2×2 linear systems of equations given by

$$\begin{pmatrix} I - ka_{11} J_1(U_j^{n,1}) & -ka_{12} J_1(U_j^{n,2}) \\ -ka_{21} J_1(U_j^{n,1}) & I - ka_{22} J_1(U_j^{n,2}) \end{pmatrix} \begin{pmatrix} v_{j+1}^{n,1} \\ v_{j+1}^{n,2} \end{pmatrix} + \mathbf{b} = \begin{pmatrix} r_1 \\ r_2 \end{pmatrix}, \tag{12}$$

and

$$\begin{pmatrix} I - ka_{11} J_2(U_j^{n,1}) & -ka_{12} J_2(U_j^{n,2}) \\ -ka_{21} J_2(U_j^{n,1}) & I - ka_{22} J_2(U_j^{n,2}) \end{pmatrix} \begin{pmatrix} w_{j+1}^{n,1} \\ w_{j+1}^{n,2} \end{pmatrix} + \mathbf{b} = \begin{pmatrix} q_1 \\ q_2 \end{pmatrix}, \tag{13}$$

where $J_1(\phi)\psi = \Theta\psi + Q(\psi,\phi)$, $J_2(\phi)\psi = -\Theta\psi + Q(\psi,\phi)$, and $v_j^{n,i} = H_j^{n,i} + U_j^{n,i}$, $w_j^{n,i} = H_j^{n,i} - U_j^{n,i}$, $i = 1, 2$.

Upon choosing a basis for S_h, it becomes apparent that (12), (13) represent two $2N \times 2N$ ($N = \dim S_h$) linear systems for the coefficients of the Newton iterates. The following device was used to uncouple the two operator equations in each system. Evaluating all four entries on the matrices A_1, A_2 at a point $U^* \in S_h$ defined by $U^* = \frac{1}{2}(U_0^{n,1} + U_0^{n,2})$ (which makes the operators in the entries of these elements independent of j and allows them to commute with each other), we may then write (12) and (13), respectively as

$$\begin{pmatrix} I - ka_{11}J_1(U^*) & -ka_{12}J_1(U^*) \\ -ka_{21}J_1(U^*) & I - ka_{22}J_1(U^*) \end{pmatrix} \begin{pmatrix} v_{j+1}^{n,1} \\ v_{j+1}^{n,2} \end{pmatrix} = \widetilde{\mathbf{r}} - \mathbf{b}, \tag{14}$$

and

$$\begin{pmatrix} I - ka_{11}J_2(U^*) & -ka_{12}J_2(U^*) \\ -ka_{21}J_2(U^*) & I - ka_{22}J_2(U^*) \end{pmatrix} \begin{pmatrix} w_{j+1}^{n,1} \\ w_{j+1}^{n,2} \end{pmatrix} = \widetilde{\mathbf{q}} - \mathbf{b}, \tag{15}$$

where

$$\widetilde{\mathbf{r}} = \begin{pmatrix} H^n + U^n \\ H^n + U^n \end{pmatrix} - k \begin{pmatrix} a_{11} & a_{12} \\ a_{21} & a_{22} \end{pmatrix} \begin{pmatrix} Q(H_j^{n,1}, U_j^{n,1}) + \frac{1}{2}Q(U_j^{n,1}) \\ Q(H_j^{n,2}, U_j^{n,2}) + \frac{1}{2}Q(U_j^{n,2}) \end{pmatrix}$$
$$-k \begin{pmatrix} a_{11} & a_{12} \\ a_{21} & a_{22} \end{pmatrix} \begin{pmatrix} J_1(U^*) - J_1(U_j^{n,1}) & 0 \\ 0 & J_1(U^*) - J_1(U_j^{n,2}) \end{pmatrix} \begin{pmatrix} v_{j+1}^{n,1} \\ v_{j+1}^{n,2} \end{pmatrix},$$

and

$$\widetilde{\mathbf{q}} = \begin{pmatrix} H^n - U^n \\ H^n - U^n \end{pmatrix} - k \begin{pmatrix} a_{11} & a_{12} \\ a_{21} & a_{22} \end{pmatrix} \begin{pmatrix} Q(H_j^{n,1}, U_j^{n,1}) - \frac{1}{2}Q(U_j^{n,1}) \\ Q(H_j^{n,2}, U_j^{n,2}) - \frac{1}{2}Q(U_j^{n,2}) \end{pmatrix}$$
$$-k \begin{pmatrix} a_{11} & a_{12} \\ a_{21} & a_{22} \end{pmatrix} \begin{pmatrix} J_2(U^*) - J_2(U_j^{n,1}) & 0 \\ 0 & J_2(U^*) - J_2(U_j^{n,2}) \end{pmatrix} \begin{pmatrix} w_{j+1}^{n,1} \\ w_{j+1}^{n,2} \end{pmatrix},$$

for $j \geqslant 0$. This form immediately suggests an iterative scheme for approximating $v_{j+1}^{n,i}$ and $w_{j+1}^{n,i}$, $i = 1, 2$. This scheme generates *inner* iterates denoted by $v_{j+1}^{n,i,\ell} = H_{j+1}^{n,i,\ell} + U_{j+1}^{n,i,\ell}$ and $w_{j+1}^{n,i,\ell} = H_{j+1}^{n,i,\ell} - U_{j+1}^{n,i,\ell}$ for given n, i, j and $\ell = 0, 1, 2, \ldots$, (here $v_{j+1}^{n,i,\ell}$ and $w_{j+1}^{n,i,\ell}$ approximate $v_{j+1}^{n,i}$ and $w_{j+1}^{n,i}$ respectively) that are found recursively from the equations

$$\begin{pmatrix} I - ka_{11}J_1(U^*) & -ka_{12}J_1(U^*) \\ -ka_{21}J_1(U^*) & I - ka_{22}J_1(U^*) \end{pmatrix} \begin{pmatrix} v_{j+1}^{n,1,\ell+1} \\ v_{j+1}^{n,2,\ell+1} \end{pmatrix} = \begin{pmatrix} r_{j+1}^{n,1,\ell} \\ r_{j+1}^{n,2,\ell} \end{pmatrix}, \tag{16}$$

and

$$\begin{pmatrix} I - ka_{11}J_2(U^*) & -ka_{12}J_2(U^*) \\ -ka_{21}J_2(U^*) & I - ka_{22}J_2(U^*) \end{pmatrix} \begin{pmatrix} w_{j+1}^{n,1,\ell+1} \\ w_{j+1}^{n,2,\ell+1} \end{pmatrix} = \begin{pmatrix} q_{j+1}^{n,1,\ell} \\ q_{j+1}^{n,2,\ell} \end{pmatrix}, \tag{17}$$

for $\ell \geqslant 1$, where, for $i = 1, 2$

$$r_{j+1}^{n,i,\ell} = H^n + U^n - k \sum_{m=1}^{2} a_{im} \left(Q(H_j^{n,i}, U_j^{n,i} - U_{j+1}^{n,i,\ell}) + \frac{1}{2}Q(U_j^{n,i}) + \left(J_1(U^*) - J_1(U_j^{n,i}) \right) v_{j+1}^{n,i,\ell} \right)$$

$$q_{j+1}^{n,i,\ell} = H^n - U^n - k\sum_{m=1}^{2} a_{im}\left(Q(H_j^{n,i}, U_j^{n,i} - U_{j+1}^{n,i,\ell}) - \frac{1}{2}Q(U_j^{n,i}) + \left(J_2(U^*) - J_2(U_j^{n,i})\right) w_{j+1}^{n,i,\ell}\right).$$

The linear systems (16), (17) can be solved efficiently as follows: Since $a_{12}a_{21} < 0$, it is possible, upon scaling the matrix on the left-hand sides by a diagonal similarity transformation, to write them as

$$\begin{pmatrix} I - \frac{1}{4}kJ_1(U^*) & kJ_1(U^*)/4\sqrt{3} \\ -kJ_1(U^*)/4\sqrt{3} & I - \frac{1}{4}kJ_1(U^*) \end{pmatrix} \begin{pmatrix} v_{j+1}^{n,1,\ell+1} \\ \mu v_{j+1}^{n,2,\ell+1} \end{pmatrix} = \begin{pmatrix} r_{j+1}^{n,1,\ell} \\ \mu r_{j+1}^{n,2,\ell} \end{pmatrix}, \tag{18}$$

and

$$\begin{pmatrix} I - \frac{1}{4}kJ_2(U^*) & kJ_2(U^*)/4\sqrt{3} \\ -kJ_2(U^*)/4\sqrt{3} & I - \frac{1}{4}kJ_2(U^*) \end{pmatrix} \begin{pmatrix} w_{j+1}^{n,1,\ell+1} \\ \mu w_{j+1}^{n,2,\ell+1} \end{pmatrix} = \begin{pmatrix} q_{j+1}^{n,1,\ell} \\ \mu q_{j+1}^{n,2,\ell} \end{pmatrix}, \tag{19}$$

where $\mu = 2 - \sqrt{3}$. These systems are equivalent to the two uncoupled complex $N \times N$ systems

$$(I - k\beta J_i(U^*))\, Z_i = R_i, \quad i = 1, 2, \tag{20}$$

where $\beta = \frac{1}{4} + \mathrm{i}/4\sqrt{3}$, and where Z_i and R_i are complex-valued functions with real and imaginary parts in S_h, depending upon n, ℓ and j, defined by $Z_1 = v_{j+1}^{n,1,\ell+1} + \mathrm{i}\mu v_{j+1}^{n,2,\ell+1}$, $R_1 = r_{j+1}^{n,1,\ell} + \mathrm{i}\mu r_{j+1}^{n,2,\ell}$ and $Z_2 = w_{j+1}^{n,1,\ell+1} + \mathrm{i}\mu w_{j+1}^{n,2,\ell+1}$, $R_2 = q_{j+1}^{n,1,\ell} + \mathrm{i}\mu q_{j+1}^{n,2,\ell}$.

In practice, only a finite number of outer and inner iterates are computed at each time step. Specifically, for $i = 1, 2$, $n \geqslant 0$, we compute approximations to the outer iterates $v_j^{n,i}, w_j^{n,i}$ for $j = 1, \ldots, J_{\text{out}}$, for some small positive integer J_{out}. For each $j, 0 \leqslant j \leqslant J_{\text{out}} - 1$, $v_{j+1}^{n,i}$ and $w_{j+1}^{n,i}$ are approximated by the last inner iterates $v_{j+1}^{n,i,J_{\text{inn}}}$, $w_{j+1}^{n,i,J_{\text{inn}}}$ of the sequences of inner iterates $v_{j+1}^{n,i,\ell}$, $w_{j+1}^{n,i,\ell}$ that satisfy linear systems of the form (20). In practice, J_{inn} and J_{out} are such that

$$\left(\sum_{k=1}^{2}\left(\|U_{j+1}^{n,k,\ell+1} - U_{j+1}^{n,k,\ell}\|_{\ell_2}^2 + \|H_{j+1}^{n,k,\ell+1} - H_{j+1}^{n,k,\ell}\|_{\ell_2}^2\right)\right)^{1/2} \leqslant \varepsilon,$$

and

$$\left(\sum_{k=1}^{2}\left(\|U_{j+1}^{n,k} - U_j^{n,k}\|_{\ell_2}^2 + \|H_{j+1}^{n,k} - H_j^{n,k}\|_{\ell_2}^2\right)\right)^{1/2} \leqslant \varepsilon,$$

where $\|v\|_{\ell_2}$ denotes the Euclidean norm of the coefficients of $v \in S_h$ with respect to the basis of S_h, and ε is usually taken to be 10^{-14} or 10^{-13}.

Given H^n, U^n, the required starting values $H_0^{n,i}, U_0^{n,i}$ for the (outer) Newton iteration are computed by extrapolation from previous values as $H_0^{n,i} = \sum_{\mu=0}^{3} \alpha_{\mu,i} H^{n-\mu}$ and $U_0^{n,i} = \sum_{\mu=0}^{3} \beta_{\mu,i} U^{n-\mu}$ for $i = 1, 2$, where the coefficients $\alpha_{j,i}, \beta_{j,i}$ are such that $H_0^{n,1}$ and $U_0^{n,1}$ are the values at $t = t^{n,i}$ of the Lagrange interpolating polynomial of degree at most 3 in t that interpolates to the data H^{n-j} and U^{n-j} at the four points t^{n-j}, $0 \leqslant j \leqslant 3$ respectively. (If $0 \leqslant n \leqslant 2$, we use the same linear combination, putting $U^j = U^0$ and $H^j = H^0$ if $j < 0$. Here, $U^0 = \Pi_h u_0$, $H^0 = \Pi_h \eta_0$).

Analogous numerical schemes may be readily derived for the coupled KdV systems (2) and (3) as well.

3. Errors of the numerical method

Since a rigorous error analysis of the fully discrete scheme (8)–(9) approximating the coupled KdV system is still lacking, we performed an experimental investigation of its orders of convergence. We

compared the numerical solution with an exact travelling wave solution of (1) derived in [8], valid for $x \in \mathbb{R}$ and given, for $\rho > 0$, by

$$\begin{aligned} \eta(x,t) &= -\tfrac{1}{2}(1+\tfrac{1}{6}\rho) + \tfrac{1}{4}\rho \mathrm{sech}^2\left(\tfrac{1}{2}\sqrt{\rho}(x-c_s t)\right), \\ u(x,t) &= -\tfrac{\sqrt{2}}{2}(1+\tfrac{1}{6}\rho) + c_s + \tfrac{1}{2\sqrt{2}}\rho \mathrm{sech}^2\left(\tfrac{1}{2}\sqrt{\rho}(x-c_s t)\right). \end{aligned} \tag{21}$$

In (21) we took $c_s = 1$ and $\rho = 30$ and solved numerically the initial-periodic boundary value problem for (1) on the spatial interval $[-5, 5]$ taking (21) for $t = 0$ as initial condition; both η and u differ from their constant, large $|x|$ asymptotic value by an amount of $O(10^{-11})$ at the endpoints $x = \pm 5$ of the interval and may be used as approximately periodic initial data. We integrated the system using cubic and quintic splines on a uniform mesh with $h = 10/N$ up to $t = 1$ with time step $k = 1/M$. In these computations, in the case of cubic splines, we observed that the error tolerances mentioned in Section 2 were met if we took $J_{\text{out}} = 2$, and $J_{\text{inn}} = 4$ or 5 for the first and $J_{\text{inn}} = 1$ for the second outer iteration. (More outer and inner iterations were needed in the first three time steps due to lack of backward steps for the extrapolations (26)). For quintic splines we observed that it was necessary to use $J_{\text{out}} = 2$ or 3 (mostly 2) coupled with $J_{\text{inn}} = 4$–5 for the first, $J_{\text{inn}} = 1$–3 for the second, and $J_{\text{inn}} = 1$ for the third outer iteration. We computed the discrete maximum error at $t = 1$ for η as $ME_\eta = \max_i |H^M(x_i) - \eta(x_i, 1)|$ and the normalized L^2 error as $LE_\eta(t^n) = \|H^n - \eta(\cdot, t^n)\|/\|\eta(\cdot, 0)\|$ for $t^n = 1$, with analogous formulas for u.

In order to investigate the spatial order of convergence of the scheme we took sufficiently small timesteps (large enough M) and computed as usual experimental values of the rate of convergence as $\log(E_i/E_{i-1})/\log(h_i/h_{i-1})$, where E_i was the error obtained with spatial meshlength h_i. The results, for cubic and quintic splines, are shown in Tables 1 and 2, respectively.

Table 1
Spatial rates of convergence (Cubic Splines)

N	M	$ME_\eta(t^n)$	Rate	$LE_\eta(t^n)$	Rate	$ME_u(t^n)$	Rate	$LE_u(t^n)$	Rate
160	500	1.782e-4		7.193e-6		2.498e-4		8.341e-6	
200	500	6.737e-5	4.36	2.464e-6	4.80	9.480e-5	4.34	2.949e-6	4.66
320	500	9.439e-6	4.18	3.196e-7	4.35	1.332e-5	4.18	3.940e-7	4.28
400	500	3.789e-6	4.09	1.273e-7	4.13	5.354e-6	4.09	1.576e-7	4.11
640	1600	5.663e-7	4.04	1.895e-8	4.05	8.005e-7	4.04	2.352e-8	4.05
800	3200	2.308e-7	4.02	7.726e-9	4.02	3.263e-7	4.02	9.590e-9	4.02
1024	3200	8.557e-8	4.02	2.869e-9	4.01	1.210e-7	4.02	3.561e-9	4.01

Table 2
Spatial rates of convergence (Quintic Splines)

N	M	$ME_\eta(t^n)$	Rate	$LE_\eta(t^n)$	Rate	$ME_u(t^n)$	Rate	$LE_u(t^n)$	Rate
100	800	9.269e-5		3.533e-6		1.339e-4		4.329e-6	
160	800	2.671e-6	7.55	9.906e-8	7.60	3.779e-6	7.59	1.230e-7	7.58
200	800	5.924e-7	6.75	2.155e-8	6.84	8.383e-7	6.75	2.675e-8	6.84
250	800	1.396e-7	6.48	4.966e-9	6.58	1.978e-7	6.47	6.165e-9	6.58
320	800	2.918e-8	6.34	1.027e-9	6.39	4.167e-8	6.31	1.274e-9	6.39
400	1600	7.462e-9	6.11	2.544e-10	6.25	1.058e-8	6.14	3.156e-10	6.26
500	1600	1.888e-9	6.16	6.533e-11	6.09	2.701e-9	6.12	7.985e-11	6.16

The tables confirm the expected theoretical spatial rate of convergence $r = 4$ for cubic and $r = 6$ for quintic splines. To investigate experimentally the temporal order of convergence, whose expected theoretical value is of course four, we computed with quintic splines taking $h = \frac{10}{N}$ with values of N shown in Table 3, and $k = h/2$. In this range of parameters h^6 is about three orders of magnitude smaller than k^4 and we expect the temporal component of the error to be the dominant one. We approximated the temporal rate as $\log(E_i/E_{i-1})/\log(k_i/k_{i-1})$. The results of Table 3 yield approximately the expected theoretical value 4.

Table 3
Time rates of convergence (Quintic Splines)

N	$ME_\eta(t^n)$	Rate	$LE_\eta(t^n)$	Rate	$ME_u(t^n)$	Rate	$LE_u(t^n)$	Rate
500	4.240e-5		4.124e-4		1.235e-7		1.805e-6	
1000	2.320e-6	4.19	2.384e-5	4.11	7.829e-9	3.98	1.093e-7	4.05
1250	9.507e-7	4.00	9.650e-6	4.05	2.874e-9	4.49	4.002e-8	4.50
1500	4.580e-7	4.01	4.597e-6	4.07	1.432e-9	3.82	2.007e-8	3.79
2000	1.445e-7	4.01	1.487e-6	3.92	4.305e-10	4.18	5.624e-9	4.42

In the case of the symmetric coupled KdV system (2), the conservation of the $L^2 \times L^2$ norm of the solution allows the rigorous derivation of optimal-order L^2 error estimates using the periodic spline *quasi-interpolant* as was done for the KdV equation in [7]. The proofs appear in [13]. Numerical experiments confirm optimal-order errors of $O(k^4 + h^r)$ in this case as well.

Although the exact solution (21) is not a solitary wave, it may be used for testing the accuracy of numerical solutions of problems with solitary-wave type solutions. To this effect, we computed the numerical solution of the initial-periodic boundary value problem for (1) using $h = 10^{-2}$, $k = 10^{-3}$, and (21) with $\rho = 30$, $c_s = 1$ on $[-5, 5]$ as before as an exact solution. In addition to the normalized L^2 error defined previously, we computed some other types of error indicators that are pertinent to the approximation of solitary waves, [7]. Specifically, at $t = t^n$, we computed the (normalized) *amplitude error* $AE_\eta(t^n) = \left|\frac{\eta_{\max} - H^n(x^*)}{\eta_{\max}}\right|$, where $\eta_{\max}$ is the maximum value of the η profile (equal to 4.5 in our case) and x^* is the point where H^n achieves its maximum. This point is found by applying Newton's method to the equation $\frac{d}{dx}H^n(x) = 0$ using a few iterations, and, as initial value, the quadrature node where H^n has a maximum. We also define an L^2 based, (normalized) *shape error* as $SE_\eta(t^n) = \inf_\tau \frac{\|H^n - \eta(\cdot,\tau)\|}{\|\eta(\cdot,0)\|}$, by first computing τ^* as the point near t^n where $\frac{d}{d\tau}\xi^2(\tau^*) = 0$, with $\xi(\tau) = \|H^n - \eta(\cdot,\tau)\|/\|\eta(\cdot,0)\|$, using Newton's method with a few iterations and $\tau^0 = t^n - k$ as initial guess. We then set $SE_\eta(t^n) = \xi(\tau^*)$; the associated *phase error* is $PE_\eta(t^n) = \tau^* - t^n$. We define the corresponding errors of u similarly. Tables 4 and 5 show the evolution of these errors up to $t^n = 6$ for cubic and quintic splines, respectively.

Table 4
Amplitude, L^2, Shape and Phase errors (Cubic Splines)

t^n	$AE_\eta(t^n)$	$AE_u(t^n)$	$LE_\eta(t^n)$	$LE_u(t^n)$	$SE_\eta(t^n)$	$SE_u(t^n)$	$PE_\eta(t^n)$	$PE_u(t^n)$
2	2.080e-8	1.797e-8	3.159e-9	1.795e-8	3.159e-9	3.917e-9	2.628e-12	-1.898e-11
4	2.133e-8	1.847e-8	4.802e-9	2.520e-8	4.680e-9	4.082e-9	-7.704e-10	-5.525e-10
6	4.992e-8	4.243e-8	7.710e-8	5.656e-8	7.677e-8	2.530e-8	-5.103e-9	8.489e-10

It should be noted that for this problem the numerical solution degenerates for larger values of t. For example, the L^2 errors increase with time and become $O(1)$ at about $t = 15.1$ for cubic splines and at about $t = 15.9$ for quintic. (The invariants $I1$, $I2$, $I3$ and the Hamiltonian H remain constant to 9 digits

Table 5
Amplitude, L^2, Shape and Phase errors (Quintic Splines)

t^n	$AE_\eta(t^n)$	$AE_u(t^n)$	$LE_\eta(t^n)$	$LE_u(t^n)$	$SE_\eta(t^n)$	$SE_u(t^n)$	$PE_\eta(t^n)$	$PE_u(t^n)$
2	8.398e-11	4.122e-11	7.497e-11	1.763e-10	5.057e-11	2.990e-11	-3.970e-11	-3.692e-11
4	3.243e-11	4.598e-11	8.797e-10	8.986e-10	8.637e-10	3.086e-10	-1.197e-10	-9.344e-11
6	3.884e-9	1.455e-9	1.988e-8	1.515e-8	1.969e-8	6.934e-9	2.000e-9	1.313e-9

up to about $t = 17$ for cubic splines and up to $t = 18$ for quintic). This is a large amplitude problem and it is not clear whether this loss of accuracy of the numerical solution is due to accumulation of temporal error due to some type of weak long-time instability or due to an instability or blow-up of the solution of the system. As we shall see in the sequel, this phenomenon was not observed in simulations of small amplitude solutions; these remained accurate for very large time spans.

4. Generalized solitary waves

Using the numerical scheme described in the previous two sections we performed many numerical experiments, the results of some of which appear in the companion paper II. In the course of some early experiments the initial-periodic boundary value problem for (1) was solved numerically with initial values $\eta(x,0) = 0.3\mathrm{e}^{-(x+100)^2/25}$, $u(x,0) = 0$ on $[-150, 150]$. As expected, this initial profile was resolved in two wave trains moving to opposite directions and led by solitary-like pulses. We tried to isolate a solitary wave (moving to the right) by iterative 'cleaning', cf. [3], i.e. by truncating the leading pulse, using it as new initial value, letting it propagate and distance itself from the trailing dispersive tail, truncate it again etc. (This will be described in more detail in paper II.) After seven such iterations a 'clean' at first sight solitary wave was produced, used as a new initial condition and allowed to evolve. At $t = 160$ the

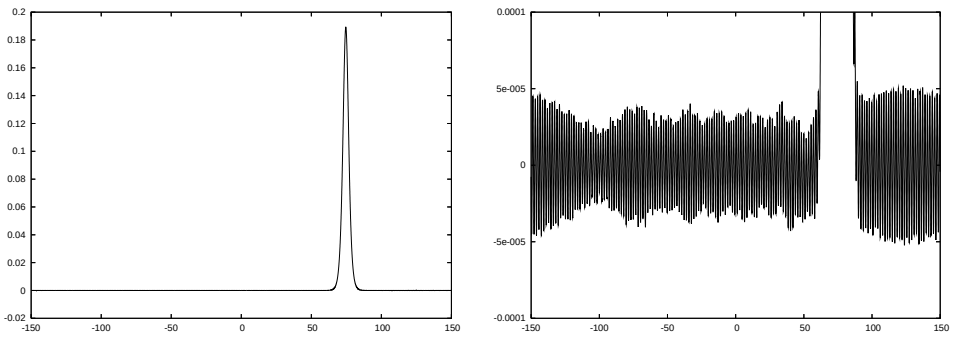

Fig. 1. Evolution of η-solitary wave of (1) produced (after 7 iterations) by iterative cleaning, $t = 160$. The figure on the right is a magnification of the one on the left.

profile of the solution is shown in Figure 1. In the magnified picture we observe that small amplitude oscillations have been produced and accompany the main pulse. These oscillations are not an artifact of the numerical scheme; they prove to be invariant under changes in (small enough) k and h, the choice of spline spaces and the time stepping method. A similar phenomenon was observed in the case of the symmetric system (2).

Such observation led us to ask whether these systems possess generalized solitary wave solutions, i.e. solitary wave pulses homoclinic to small amplitude oscillatory solutions. Such solutions are known to exist for the full Euler equations with small surface tension and other model nonlinear dispersive wave

equations, cf. e.g. [2], [10]–[12], [14], [15]. It turns out that the answer is affirmative since the vector field in $\mathbb{R}^4$ that defines the o.d.e. system corresponding to travelling wave solutions for (1)–(2) admits a $0^{2+}\mathrm{i}\omega$ resonance, [11].

We consider the system (1), and following the notation and terminology of [11], we seek travelling wave solutions of the form $\eta(x,t)=\eta(\xi)$, $u(x,t)=u(\xi)$, $\xi=x-c_st$, where we write $c_s=c+1$. Substituting into (1), integrating once, setting the integration constants equal to zero and putting $u_1=\eta$, $u_2=\eta'$, $u_3=u$, $u_4=u'$, $\left(' = \frac{d}{d\xi}\right)$ we may write the resulting equations as a dynamical system on $\mathbb{R}^4$ for $U=(u_1,u_2,u_3,u_4)^T(\xi)$, in the form $U'=V(U,c)$, i.e. as

$$\begin{aligned} u_1' &= u_2,\\ u_2' &= -6u_1+6(c+1)u_3-3u_3^2,\\ u_3' &= u_4,\\ u_4' &= 6(c+1)u_1-6u_3-6u_1u_3. \end{aligned} \tag{22}$$

Hence $U'=V(U,c)\equiv L(c)U+R(U)$, where

$$L(c)=\begin{pmatrix} 0 & 1 & 0 & 0\\ -6 & 0 & 6(c+1) & 0\\ 0 & 0 & 0 & 1\\ 6(c+1) & 0 & -6 & 0 \end{pmatrix} \quad \text{and} \quad R(U)=\begin{pmatrix} 0\\ -3u_3^2\\ 0\\ -6u_1u_3 \end{pmatrix}.$$

It is easily seen that the spectrum of $L(c)$, is the set $\left\{-\sqrt{6}\sqrt{-2-c},\sqrt{6}\sqrt{-2-c},-\sqrt{6}\sqrt{c},\sqrt{6}\sqrt{c}\right\}$. In addition, the vector field V has the following properties:

(i) $V(0,c)=0$ for all c. ($U=0$ is a 'fixed' point of the system $U'=V(U,c)$).

(ii) $SV(U,c)=-V(SU,c)$, where $S=diag\{1,-1,1,-1\}$. (V is 'reversible').

(iii) The spectrum of $L(0)$ is $\{0,\pm\mathrm{i}\omega\}$, $\omega=2\sqrt{3}$. The eigenvalue 0 is double and non-semisimple. The corresponding basis of $\mathbb{C}^4$ is given by

$$\phi_0=(1,0,1,0)^T,\ \phi_1=(0,1,0,1)^T,\ \phi_+=(\frac{\mathrm{i}}{2\sqrt{3}},-1,-\frac{\mathrm{i}}{2\sqrt{3}},1)^T,\ \phi_-=(-\frac{\mathrm{i}}{2\sqrt{3}},-1,\frac{\mathrm{i}}{2\sqrt{3}},1)^T,$$

where $\phi_0,\phi_\pm$ are eigenvectors corresponding to the eigenvalues $0,\pm\mathrm{i}\omega$, respectively, and ϕ_1 is a generalized eigenvector of 0.

(iv) $S\phi_0=\phi_0$.

(v) Denoting by $\left\{\phi_0^*,\phi_1^*,\phi_+^*,\phi_-^*\right\}$ the corresponding dual basis, (so that e.g. $\phi_1^*=(0,1/2,0,1/2)^T$) we have that $c_{10}:=\langle\phi_1^*,D^2_{cu}V(0,0)\phi_0\rangle>0$ and $c_{20}:=\frac{1}{2}\langle\phi_1^*,D^2_{uu}V(0,0)[\phi_0,\phi_0]\rangle\neq 0$. (For (1) $c_{10}=6$ and $c_{20}=-9/2$).

By Theorem 7.1.1 of [11] we may infer from these properties that there exist constants $\sigma,\kappa_3,\kappa_2,\kappa_1,\kappa_0>0$, such that, for $c>0$ small enough, the vector field $V(U,c)$ admits near $U=0$:

(a) A one parameter family of periodic orbits $p_{\kappa,c}$ of arbitrary small amplitude $\kappa\in[0,\kappa_3 c]$.

(b) For every $\kappa\in[\kappa_1\, c\, \mathrm{e}^{\frac{-\omega(\pi-\sigma(c_{10}c)^{3/10})}{\sqrt{c_{10}c}}},\kappa_2 c]$, a pair of reversible (i.e. such that $U(\xi)=SU(-\xi)$) homoclinic connections to $p_{\kappa,c}$ with one loop.

(c) No reversible homoclinic connections to $p_{\kappa,c}$ with one loop if $\kappa\in[0,\kappa_0\, c\, \mathrm{e}^{\frac{-\pi\omega}{\sqrt{c_{10}c}}})$.

We will call *generalized solitary waves* the profiles that are homoclinic to small amplitude periodic solutions. It is not hard to see that the symmetric system (2) also satisfies conditions (i)–(v) (with $c_{20}=-6$). We conclude that both systems possess generalized solitary waves of small amplitude and speed $c_s=1+c$,

$c > 0$ small, which decay to exponentially small oscillatory solutions; there is a critical size of the amplitude of the latter, below of which there exist no generalized solitary waves.

In order to construct numerically such generalized solitary waves we solve the o.d.e. system (22) in the case of (1) (and the analogous system for (2)) imposing periodic boundary conditions on u_i at the end points of the interval $[-L, L]$ for several L, given $c > 0$ small. Starting from an initial guess and using continuation we employ as a solver the MATLAB® function `bvp4c`, which implements a collocation method based on the 3-stage Lobatto IIIa quadrature rule. The mesh selection and the error control of the function are based on the `residuals` of the C^1 numerical solution that it provides.

In the case of (1), if we take $c = 0.2$ and initial guess sech^2-profiles for u_i and a specific L, we observe

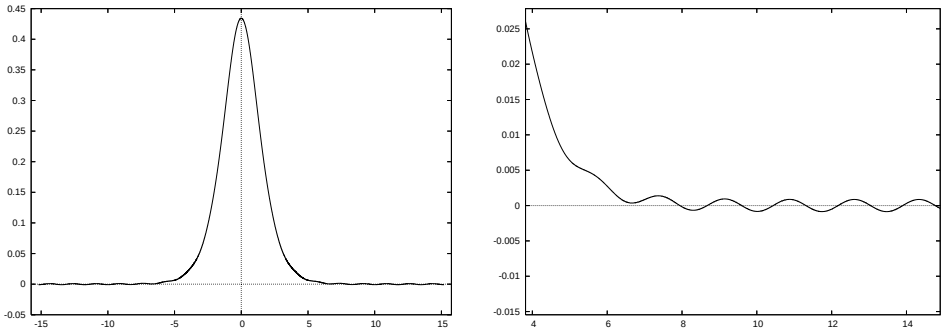

Fig. 2. Profile of the η-generalized solitary wave for the system (1) with ripples with minimum amplitude $\min \alpha = 0.000860$, $L = 15.2$.

that the numerical method is able to converge, with residuals of $O(10^{-7})$ or better, to the η-profile shown in Figure 2. (The u-profile has a similar form). In Figure 2 the generalized solitary wave consists of a main 'solitary' pulse connected to a small amplitude periodic profile (ripples). The amplitude of the small oscillations varies with L as Figure 3 shows. In Figure 3 we have plotted, for $c = 0.2$, the amplitude of

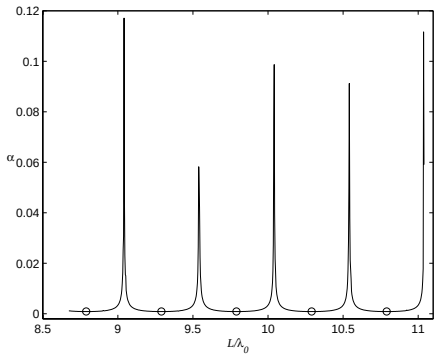

Fig. 3. Amplitude of the oscillations α vs L/λ_0. The first '$\circ$' corresponds to the solution plotted in Figure 2. (System (1))

the small oscillations versus L/λ_0, where $\lambda_0 = 2\pi/k$ is the wavelength corresponding to the wave number $k = \sqrt{6(c_s + 1)} = \sqrt{6(c + 2)}$ obtained from the dispersion relation for the linearized system (1). For $c = 0.2$ this gives $\lambda_0 \cong 1.72939$. (We have solved the o.d.e. system for $L = 15 + 0.05i$, $i = 0, \ldots, 100$ and computed the amplitude of the associated ripples.) The minimum amplitude $\min \alpha$ occurs approximately at $\frac{L}{\lambda_0} = \frac{n}{2} + \frac{1}{4}$, $n = 17, 18, \ldots$, and is constant to six decimal digits and equal to 0.000860. (Figure 2 corresponds to $L = 15.2$, i.e. to the value where $\min \alpha$ first occurs. Computing with different L's

corresponding to the minimum amplitude ripples – denoted by small circles in Figure 3 – will produce again Figure 2 extended with ripples to the right and left.) The wavelength of the ripples in Figure 2 is equal to about $\lambda \cong 1.73$, which is a good approximation of the wavelength λ_0 of the linearized problem. The maximum values of the amplitude occur near the values $\frac{L}{\lambda_0} = \frac{n+1}{2}$, $n = 17, 18, \ldots$; the o.d.e. code loses accuracy near these points and the maximum values of α shown in Figure 3 are not trustworthy. (Similar observations have been previously made by Michallet and Dias, [12], in their numerical study of generalized solitary waves of a two-fluid system.)

The analogous o.d.e. system that corresponds to the symmetric system (2) is much easier to solve numerically as evidenced by the smaller residuals (of $O(10^{-8})$ or better) that `bvp4c` returns. In this case, we were able to compute generalized solitary waves with $c = 0.2$ and $c = 0.3$ and observed that the amplitude of the ripples increases with c: When $c = 0.2$ we obtained $\min \alpha = 0.0012265$, while when $c = 0.3$, $\min \alpha = 0.0074614$. The maximum values also increase.

In Figure 4 we compare the amplitude of the ripples for $c = 0.2$ and the profile of the generalized solitary wave with minimum ripple amplitude for the two coupled KdV systems (1) and (2).

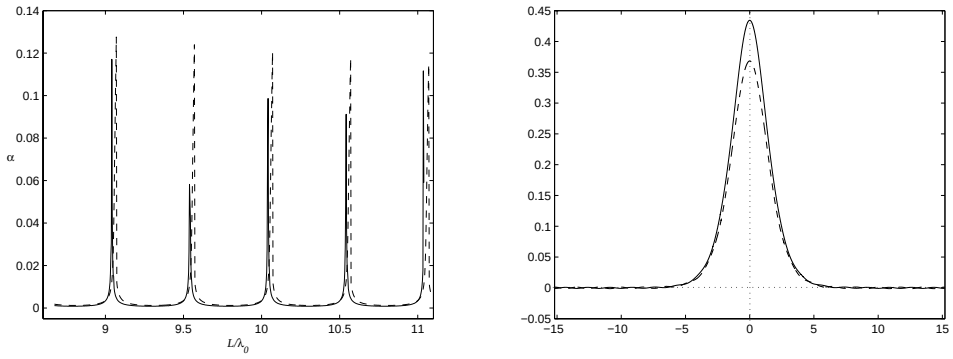

Fig. 4. Comparison of generalized solitary waves of systems (1) (solid line) and (2) (dotted line) for $c = 0.2$. Left: amplitude of ripples vs L/λ_0. Right: η-generalized solitary waves with the minimum ripples.

As a further test of the accuracy of the `bvp4c` function and the evolution code described in Sections 2 and 3, we took generalized solitary waves as initial data and let them evolve in time numerically using the evolution code. The results were quite satisfactory. Figure 5 shows the η-generalized solitary wave of the system (2) with c=0.2 in $[-15, 15]$ at $t = 0$ and at $t = 170$. During this run (with $h = 0.1$, $k = 0.01$,

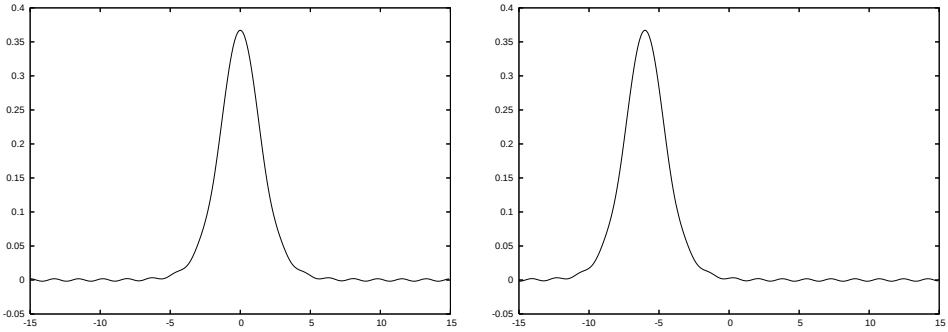

Fig. 5. Numerical integration in time of the generalized solitary wave with $c = 0.2$ for the system (2). The η-components of the solution is shown at $t = 0$ (left) and at $t = 170$ (right).

$r = 4$ up to $T = 200$) the invariant quantity $\int_{-L}^{L}(\eta^2 + u^2)dx$ had the value 0.73237518000 maintaining the eleven digits shown, while the quantities $\max \eta = 0.367190$, $\max u = 0.414506$, $c_s = 1.199999$ conserved six digits.

The analogous numerical integration in time for the system (1) was also quite accurate: Up to $T = 200$ and with $h = 0.1$, $k = 0.01$, $r = 4$ the invariant quantities $\max \eta = 0.434972$, $\max u = 0.385334$, $c_s = 1.199999$, $I_1 = 1.5702595987$, $I_2 = 1.4681669211$, $I_3 = 0.41614398659$, $H = -0.93347587389$ were conserved to the digits shown.

Let us also mention that using two or more sech^2-type, sufficiently separated pulses as initial guesses and integrating the o.d.e. system with `bvp4c` will gave *multi-humped* generalized solitary waves as Figure 6 shows for the system (1). (Similarly for the system (2)).

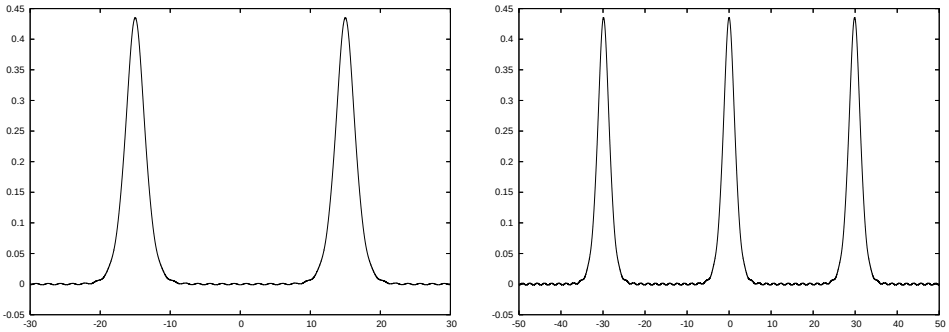

Fig. 6. η-component of generalized solitary waves with two and three humps, $c = 0.2$, for the system (1).

We finally remark that the general coupled KdV system (3) has exact solitary waves at least for $\frac{1}{12} < \tau < \frac{1}{6}$. For this range of Bond number, it has been found, cf. [9], that (3) has exact solitary waves of the form $\eta(\xi) = \eta^0 \mathrm{sech}^2(\lambda\xi)$, $u(\xi) = B\eta(\xi)$, where $\xi = x + x_0 - c_s t$, $\eta^0 = \frac{3-36\tau}{-2+12\tau}$, $\lambda = \sqrt{\eta^0}$, $B = \sqrt{2 - 12\tau}$, $c_s = \frac{2-B^2}{B}$. For other values of τ and c_s we found numerically (by solving the associated o.d.e. system with periodic boundary conditions using `bvp4c`), other types of travelling wave solutions shown in Figure 7.

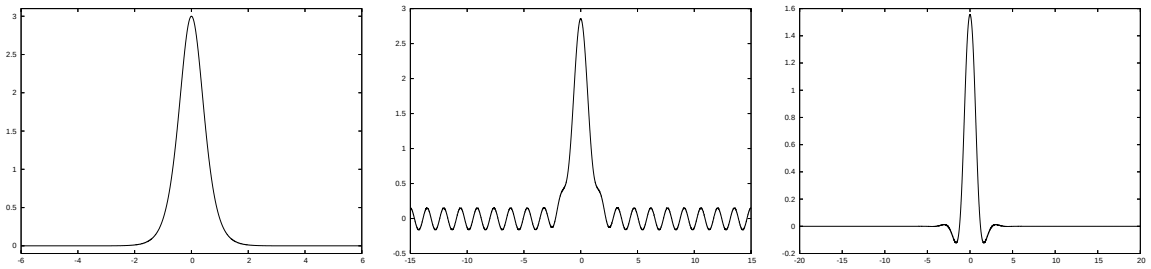

(a) (b) (c)

Fig. 7. η-component of travelling wave solutions for system (3). (a): Solitary wave, $\tau = 1/8$, $c_s = 3\sqrt{0.5}$, (b): Generalized solitary wave, $\tau = 0.01$, $c_s = 1.95$, (c): Travelling wave (kink), $\tau = 0.9$, $c_s = 2.9$.

Acknowledgments

We would like to thank Dr. D. C. Antonopoulos for early computations and observations about the oscillatory residue that remains when cleaning solitary waves for (1), cf. Figure 1, and Professors S. Venakides, A. de Bouard, G. Iooss and T. Akylas for discussions on generalized solitary waves.

References

[1] D. C. Antonopoulos, V. A. Dougalis and D. E. Mitsotakis, Theory and numerical analysis of the Bona-Smith systems of Boussinesq equations, (to appear).

[2] E. S. Belinov, R. Grimshaw and E. P. Kuznetsova, The generation of radiating waves in a singularly-perturbed Korteweg-de Vries equation, *Physica D*, 96(1993), 270–278.

[3] J. L. Bona and M. Chen, A Boussinesq system for two-way propagation of nonlinear dispersive waves, *Physica D* 116(1998), 191–224.

[4] J. L. Bona, M. Chen and J.-C. Saut, Boussinesq equations and other systems for small-amplitude long waves in nonlinear dispersive media: I. Derivation and Linear Theory, *J. Nonlinear Sci.*, 12(2002), 283–318.

[5] J. L. Bona, M. Chen and J.-C. Saut, Boussinesq equations and other systems for small-amplitude long waves in nonlinear dispersive media: II. The nonlinear theory, *Nonlinearity*, 17(2004), 925–952.

[6] J. L. Bona, T. Colin and D. Lannes, Long wave approximations for water waves, *Arch. Rational Mech. Anal.*, (to appear).

[7] J. L. Bona, V. A. Dougalis, O. A. Karakashian and W. R. McKinney, Conservative, high-order numerical schemes for the generalized Korteweg-de Vries equation, *Trans. R. Soc. Lond.* A, 351(1995), 107–164.

[8] M. Chen, Exact travelling-wave solutions to bi-directional wave equations, *Int. J. Theor. Phys.* 37(1998), 1547–1567.

[9] P. Daripa and R. Dash, A class of model equations for bi-directional propagation of capillary-gravity waves, *Int. J. Engineering Sci.* 41(2003), 201–218.

[10] F. Dias and G. Iooss, Water-waves as a spatial dynamical system, *Handbook for Mathematical Fluid Dynamics*, chap. 10 p. 443–499. S. Friedlander, D. Serre Eds., Elsevier 2003.

[11] E. Lombardi, Oscillatory integrals and phenomena beyond all algebraic orders, with applications to homoclinic orbits in reversible systems. *Lecture Notes in Mathematics*, 1741, Springer-Verlag, Berlin, (2000).

[12] H. Michallet and F. Dias, Numerical study of generalized interfacial waves, *Phys. Fluids* (11) 6, (1999) 1502–1511.

[13] D. E. Mitsotakis, Ph.D. Thesis, University of Athens, (in preparation).

[14] S. M. Sun, Non-existence of truly solitary waves in water with small surface tension, *Proc. R. Soc. Lond.* A (1999) 455, 2191–2228.

[15] T. S. Yang and T. R. Akylas, Weakly nonlocal gravity-capillary solitary waves, *Phys. Fluids* (6) 8, (1996) 1506–1514.